Philips J. Res. 51 (1998) 479–494

DEVICE OPERATION OF POLYMER LIGHT-EMITTING DIODES

by P.W.M. BLOM and M.J.M. DE JONG

Philips Research Laboratories, Prof. Holstlaan 4, 5656 AA Eindhoven, The Netherlands

Abstract

Easy processing and mechanical flexibility make polymer light-emitting diodes (PLEDs) suitable candidates for large-area display applications. The understanding of the device properties of PLEDs is a key ingredient for further optimization. This article reviews a device model developed at Philips Research that describes the current and light generation of PLEDs as a function of applied voltage. The model is based on experiments carried out on poly(dialkoxy-p-phenylene vinylene) devices. The combination of the experimental results and model calculations have revealed that (1) the hole current is dominated by space-charge effects and a field-dependent mobility, (2) the electron current is strongly reduced by traps, and (3) the recombination process between the injected electrons and holes is of the Langevin-type. These results explain specific device properties of PLEDs such as a bias-dependent and temperature-independent electroluminescence efficiency (photon/carrier) and indicate directions for further improvement of the device performance.

Keywords: Polymer LEDs, charge transport, device modelling.

1. Introduction

Since their discovery in 1990 polymer light-emitting diodes (PLEDs) have been considered promising candidates for large area-applications as a result of both easy processing and mechanical flexibility [1,2]. A typical PLED consists of a thin layer of undoped conjugated polymer sandwiched between two electrodes on top of a glass substrate. The polymer is spin-coated on top of a patterned indium-tin-oxide (ITO) bottom electrode which forms the anode. The cathode on top of the polymer consists of an evaporated metal layer for which Ca is used. The device operation of a PLED under forward bias is schematically indicated in Fig. 1. Electrons and holes are injected from the

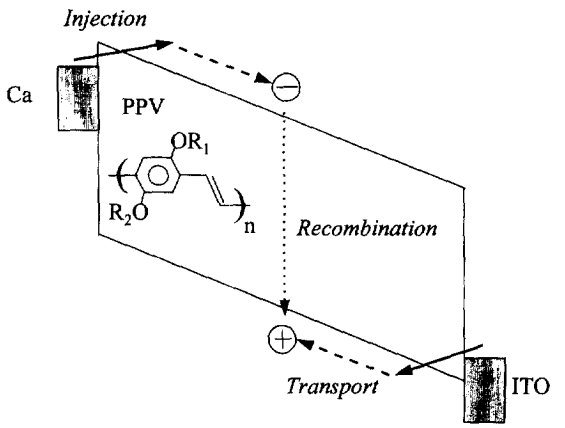

Fig. 1. Schematic band diagram of a PPV-based PLED under forward bias using ITO as a hole- and Ca as an electron injector. The inset shows the PPV used in this study with $R_1 = CH_3$ and $R_2 = C_{10}H_{21}$.

cathode and the anode, respectively, into the polymer. Driven by the applied electric field, the charge carriers move through the polymer over a certain distance until recombination takes place. The device operation of a PLED is thus determined by three processes: charge injection, charge transport, and recombination [3].

Experimentally, attention has especially been focused on PLEDs that contain the conjugated polymer poly(phenylene vinylene) (PPV) or its derivatives (see inset of Fig. 1). These devices may have an external conversion efficiency larger than 1% photons/charge carrier. Studies of the device properties of PPV-based LEDs have yielded conflicting information about which process dominates the operation of a PLED. It has been found by several groups [4,5] that the dependence of the current density J on the applied voltage V resembles that of Fowler–Nordheim tunnelling through a barrier. This suggests that the operation of a PLED is limited by the tunnelling of electrons and holes through contact barriers arising from the band offset between the polymer and the electrodes. However, quantitatively the currents predicted by the Fowler–Nordheim theory exceed the experimentally observed currents by several orders of magnitude. In spite of this discrepancy the concept of Fowler–Nordheim tunnelling became a generally accepted model in order to explain the device performance of PLEDs. Following this model the device performance of PLEDs can be improved by balancing and reducing the contact barriers of both electrons and holes. An unbalanced injection results in an excess of one carrier type and thus in a current flow which partially does not

contribute to light emission. Reduction of the contact barrier leads to a larger current and a higher light-output at equal voltage. Thus in order to obtain an efficient device the work function of the cathode and anode should both be close to the conduction and valence band of the PPV, respectively. Therefore, a low work-function metal cathode, such as Ca, and a high work function anode, such as ITO, are preferably used, as indicated in Fig. 1.

On the other hand, it has been found that the transport properties of electrons and holes in PPV are highly asymmetric. Time-of-flight measurements by Antoniades et al. [6] have shown that electrons, in contrast to holes, are severely trapped in PPV. Clearly, the resulting unbalanced electron and hole transport must affect the $J-V$ characteristics and efficiency of PLEDs. As a result of the reduced electron transport the electroluminescence is confined to a region close to the cathode. Since metallic electrodes are very efficient quenching centres for the generated electroluminescence this confinement is expected to strongly decrease the device performance.

It is important to have a model that accurately describes the device operation of PLEDs. A thorough understanding of the device characteristics of PLEDs will give insight in how to improve the performance of present and future devices. Recently, we have performed elaborate measurements and model calculations on PPV based devices. The combination of the experimental results and the calculations have revealed that the transport in our PLEDs is limited by the bulk-conduction properties of PPV and not by charge injection. The detailed results of our studies have been published in a series of papers. This paper provides a brief review and summarizes the main points.

The outline of this paper is as follows: In Sec. 2 the construction of the devices to be discussed is described. In Secs. 3 and 4 we discuss the transport properties of two types of special devices, the hole-only and electron-only devices, where only one type of charge carrier is flowing through the device. Then in Sec. 5 the properties of double-carrier devices, where both electrons and holes are injected into the PLED, are investigated. From the comparison between single- and double-carrier PLEDs information about the recombination process in a PLED is obtained. In Sec. 6 the device efficiency of a PLED is discussed. Finally, in Sec. 7 we provide some guidelines on how to further improve the device performance of our PLEDs.

2. Devices and setup

The devices that we have studied consist of a single polymer layer sandwiched between two electrodes on top of a glass substrate. The polymer is

soluble poly(dialkoxy-p-phenylenevinylene) [7], shown in the inset of Fig. 1 with R_1=CH_3 and R_2=$C_{10}H_{21}$, which is spin-coated on a patterned bottom electrode. In order to study the transport properties of holes an ITO bottom contact and an evaporated Au top contact are used. In these hole-only devices [5] the work functions of both electrodes are close to the valence band of PPV preventing electron injection from the negatively biased electrode, as indicated in the inset of Fig. 2. The transport properties of electrons have been investigated using an electron-only device consisting of a PPV layer sandwiched between two Ca electrodes. Ca has a work-function close to the conduction band of PPV, as shown in the inset of Fig. 5. Finally, for the double-carrier PLEDs ITO is used as a hole injector and Ca as an electron injector, as shown in Fig. 1. The $J-V$ measurements have been performed in a nitrogen atmosphere in a temperature range of 200 to 300 K using a HP 4145A semiconductor parameter analyser. The detection limit of our setup is about a few pA, which corresponds to $J = 10^{-6}$ A/m^2 for the electrode area of 10^{-5} m^2.

3. Hole-only devices

In Fig. 2 the $J-V$ characteristics of several ITO/PPV/Au hole-only devices are presented [8]. From the slope of the log J vs log V plot we observe that the current density J depends quadratically on the voltage V. This behaviour is characteristic for space-charge limited current (SCLC) in which case [9]

$$J = \frac{9}{8}\epsilon_0\epsilon_r\mu_p\frac{V^2}{L^3}, \tag{1}$$

with $\epsilon_0\epsilon_r$ the permittivity of the polymer, μ_p the hole mobility, and L the thickness of the device. Assuming $\epsilon_r = 3$, we find that the $J-V$ characteristics of our devices, with $L = 0.13$, 0.3, and 0.7 μm respectively, are described well by eq. (1) using $\mu_p = 5 \times 10^{-11}$ m^2/V s. The importance of the observation of space-charge limited current in our hole-only devices is that it clearly demonstrates that the hole current is bulk-limited and not injection-limited, as proposed before [4,5]. At high electric fields ($> 3 \times 10^5$ V/cm) we observe a gradual deviation from eq. (1) as demonstrated in Fig. 3 where the experimental $J-V$ characteristics of a hole-only device with $L = 0.125$ μm are plotted for six temperatures between 209 K and 296 K. The $J-V$ behaviour according to eq. (1) is also plotted at low fields as dashed lines. At higher voltages it is observed that the current density J is larger than as is expected from eq. (1). This suggests that the carrier mobility increases with electric field.

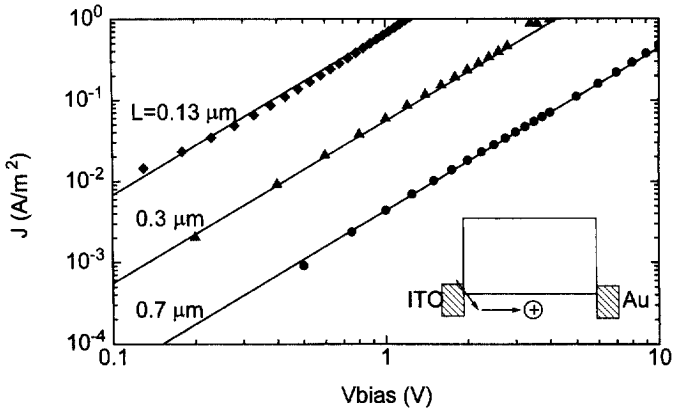

Fig. 2. Experimental and calculated (solid lines), $J-V$ characteristics of ITO/PPV/Au hole-only devices with thicknesses $L = 0.13 \cdot \mu$m (squares), $0.30\,\mu$m (triangles), and $0.70\,\mu$m (dots). The hole transport for all samples is described by SCLC [eq. (1)] with a hole mobility $\mu_p = 0.5 \times 10^{-6}$ cm^2/V s and a dielectric constant $\epsilon_r = 3$. The device structure is indicated in the inset.

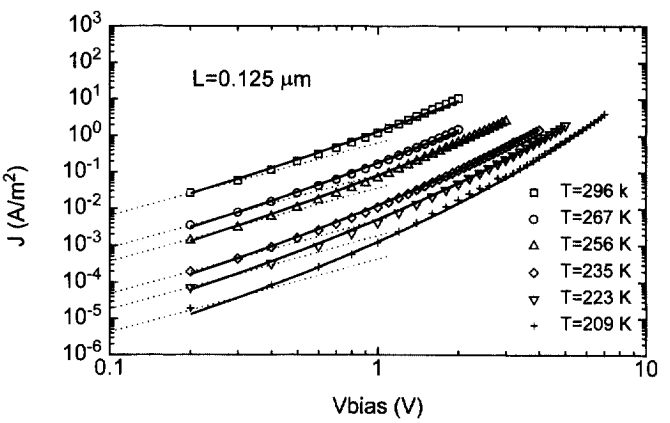

Fig. 3. Experimental $J-V$ characteristics of a ITO/PPV/Au hole-only device with thickness $L = 0.125\,\mu$m for various temperatures. In the low-field part the predicted $J-V$ characteristics (dotted lines) according to the conventional SCLC model [eq. (1)] are shown. Also shown are the calculated $J-V$ characteristics as predicted by a SCLC model using the field dependent mobility defined by eqs. (2) and (3) using $\Delta = 0.48$ eV, $G = 2.9 \times 10^{-5}$ eV(V/m)$^{-1/2}$ and $T_0 = 600$ K.

In 1970 Pai [11] demonstrated by time-of-flight (TOF) measurements that at high electric field E the mobility of photo-injected holes in poly(N-vinylcarbazole) (PVK) can be described by

$$\mu_p(E) = \mu_0 \exp\left(-\frac{\Delta}{kT}\right) \exp(\gamma\sqrt{E}), \tag{2}$$

with a temperature independent prefactor μ_0, activation energy Δ, Boltzmann's constant k, and temperature T. The field dependence (2) through the coefficient γ is comparable to the Poole–Frenkel effect [12]. However, it was soon recognized that the physical origin of eq. (2), which appears to be applicable to a large variety of molecular doped polymers as well as molecular glasses, is not the presence of traps, but it is related to the intrinsic charge transport in disordered materials [13]. Recently, time-of-flight measurements [14] on a substituted derivative poly(1,4-phenylene-1,2-diphenoxyphenyl vinylene) of PPV also provided mobilities in agreement with eq. (2). This supports our assumption that the deviations from eq. (1) are due to a field dependent mobility.

In order to describe the hole conduction in PPV at both low and high fields, we combine the SCLC, eq. (1), with the field-dependent mobility μ_p of eq. (2). As stated above, at low voltages the $J-V$ characteristics of the holes are well described by the conventional SCLC of eq. (1). This provides a direct measurement of the zero-field mobility $\mu_0 \exp(-\Delta/kT)$. The calculated current at high voltages is only dependent on the coefficient γ. We observe that the hole mobility is thermally activated and that it decreases over more than three orders of magnitude while going from $T = 296\,\mathrm{K}$ to $209\,\mathrm{K}$. The low-field mobility can be described by eq. (2), using $\Delta = 0.48\,\mathrm{eV}$ and $\mu_0 = 3.5 \times 10^{-3}\,\mathrm{m^2/V\,s}$. At higher voltages we extract γ for our PPV at each temperature. Figure 4 suggests that the observed temperature dependence of γ can accurately be described by an empirical expression

$$\gamma = G\left(\frac{1}{kT} - \frac{1}{kT_0}\right). \tag{3}$$

This result has also been found in PVK by Gill [15], with $G \approx 2.7 \times 10^{-5}\,\mathrm{eV}\,(\mathrm{V/m})^{-1/2}$ and $T_0 \approx 520$ to $660\,\mathrm{K}$, depending on the molecular dopant density. For our PPV we obtain $G = 2.9 \times 10^{-5}\,\mathrm{eV(V/m)^{-1/2}}$ and $T_0 = 600\,\mathrm{K}$. In Fig. 3 it is demonstrated that the combination of SCLC and a field-dependent mobility provides an excellent agreement with the experimental $J-V$ curves in both the low- and high- voltage regime. In summary: the decrease of the thermally activated behaviour with increasing electric field is a result of the field-enhanced carrier mobility and is not due to field emission at the contact as suggested before [4,5].

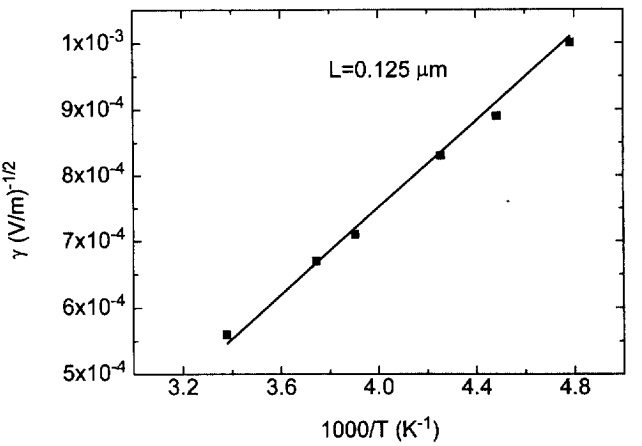

Fig. 4. Temperature dependence of the Poole–Frenkel factor γ as obtained from the high field $J-V$ characteristics of Fig. 3. Also shown is the empirical dependence (solid line) [eq. (5)] as proposed by Gill [15]. Using this empirical description we obtain for our PPV a T_0 of 600 K and a constant G of 2.9×10^{-5} eV(V/m)$^{-1/2}$, which are both in close agreement with the values reported by Gill [15] for PVK.

A microscopic theory for the observed mobility according to eqs. (2) and (3) is still lacking. Monte-Carlo simulations by Bässler [13] of hopping between sites that are subject to both positional and energetic disorder agree with eqs. (2) and (3) in a limited-field regime. Taking into account spatial correlations in the energetic disorder improves agreement with experiment [16]. A theoretical explanation for the mobility which seems to be applicable to a large class of disordered materials is highly wanted, since it would clarify the physical meaning of the invoked parameters, determined empirically here.

4. Electron-only devices

The transport properties of electrons are investigated using an electron-only device consisting of a PPV layer sandwiched between two Ca electrodes, which have a work function close to the conduction band of PPV (see inset of Fig. 5). In Fig. 5 the $J-V$ characteristics of electron-only devices with thickness $L = 0.22\,\mu$m, $0.31\,\mu$m, and $0.37\,\mu$m are shown together with the $J-V$ characteristic of a hole-only device with $L = 0.3\,\mu$m. The electron current is smaller than the hole current, especially at low bias where the difference amounts to three orders of magnitude. Furthermore, the electron current shows a very strong field-dependence which is characteristic for the trap-filled limit (TFL) in an insulator with traps [9]. For trap levels located at a single energy there

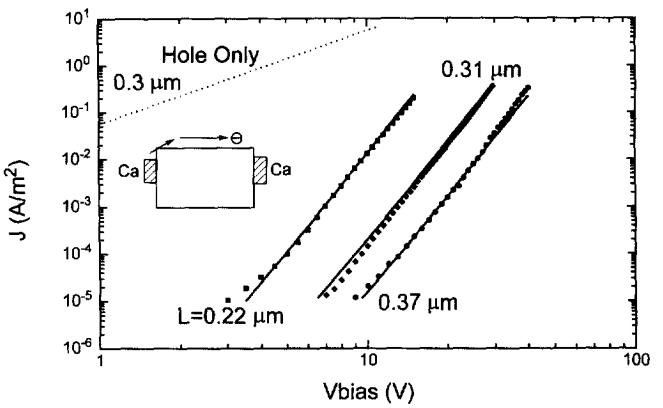

Fig. 5. Thickness dependence of the electron only $J-V$ characteristics at $L = 0.22\,\mu$m, $0.31\,\mu$m, and $0.37\,\mu$m. The solid lines represent the predicted $J-V$ characteristics according to eq. (5). For this set of samples the trap density $N_t = 1 \times 10^{18}$ cm^{-3}. For comparison also the $J-V$ characteristics of a hole-only device with thickness $L = 0.3\mu$m is shown.

is an extremely sharp transition, at which the current directly switches to the SCLC. The more gradual increase, as observed in Fig. 5, points to a distribution of trap-level energies. Actually, this is what one would expect for a disordered system, such as a spin-coated conjugated polymer. The $J-V$ characteristics in Fig. 5 are well described using an exponential distribution of traps ($\epsilon < E_c$)

$$n_t(\epsilon) = \left(\frac{N_t}{kT_t}\right) \exp\left(\frac{\epsilon - E_c}{kT_t}\right), \tag{4}$$

with $n_t(\epsilon)$ the trap density of states at energy ϵ, E_c the energy of the conduction band, N the total density of traps, and kT_t an energy characterizing the trap distribution. The trap distribution (4) implies for the $J-V$ characteristic in the TFL regime [9]

$$J = N_c e \mu_n \left(\frac{\epsilon_0 \epsilon_r}{qN_t}\right)^r \frac{V^{r+1}}{L^{2r+1}} C(r), \tag{5}$$

with $r = T_t/T$, the effective density of states in the conduction band estimated as $N_c = 2.5 \times 10^{19}$ cm^{-3}, and $C(r) = r^r(2r+1)^{r+1}(r+1)^{-r-2}$.

The $J-V$ characteristics in Fig. 5 are then determined by three parameters: the carrier mobility μ_n, the trap density N_t, and the trap distribution parameter T_t. The latter follows directly from the slope of the log J vs log V characteristic in the TFL regime, according to eq. (5), which yields $T_t = 1500$ K. Assuming [17] $\mu_p = \mu_n$, we find that $N_t = 1 \times 10^{18}$ cm^{-3}. Using these parameters we find good agreement between our experimental and theoretical results, as shown in

Fig. 5. The observed thickness dependence, which is characteristic for an exponential trap distribution, clearly proves that the electron current is determined by the bulk-transport properties of the PPV. In summary: our results confirm the severe trapping of electrons as observed in time-of-flight measurements by Antoniades et al. [6].

5. Double carrier devices

The results obtained in this study so far enable us to further investigate the relevance of the unbalanced electron and hole transport to the device efficiency of a polymer LED. Now we propose a model for the $J-V$ and efficiency versus V behaviour of a PPV based PLED taking into account the effects of both space-charge (holes) and trapping (electrons). For a double-carrier device two additional phenomena become of importance, namely recombination and charge neutralization. We will assume that the recombination is bimolecular, i.e. that its rate is proportional to the product of the electron and hole concentrations. Due to charge neutralization the *total* charge may far exceed the net charge. As a result the current density in a double-carrier device can be considerably larger than in a single-carrier device. In the simple case without traps and a field-independent mobility the double carrier current (plasma limit) is given by [9]

$$J = \left(\frac{9\pi}{8}\right)^{1/2} \epsilon_0 \epsilon_r \left(\frac{2q\mu_p\mu_n(\mu_p + \mu_n)}{\epsilon_0 \epsilon_r B}\right)^{1/2} \frac{V^2}{L^3}, \tag{6}$$

with B the bimolecular recombination constant. Upon increasing B the amount of neutralization decreases, so that J becomes smaller. The difference in current between a single- and a double-carrier device [eqs. (1) and (6)] provides direct information about the strength of the recombination process.

We compare the $J-V$ characteristics of an ITO/PPV/Au hole-only device with an ITO/PPV/Ca double injection device in Fig. 6 at various temperatures. The device thickness $L = 0.28\ \mu$m. Unfortunately, eq. (6) is not directly applicable to the experimental results of Fig. 6, since electron traps and a field-dependent mobility are not included. Therefore, we present a device model which is characterized by the current-flow equation

$$J = J_p + J_n = e\mu_p[E(x)]p(x)E(x) + e\mu_n[E(X)]n(x)E(x), \tag{7}$$

the Poisson equation

$$\frac{\epsilon_0 \epsilon_r}{e} \frac{dE(x)}{dx} = p(x) - n(x) - n_t(x), \tag{8}$$

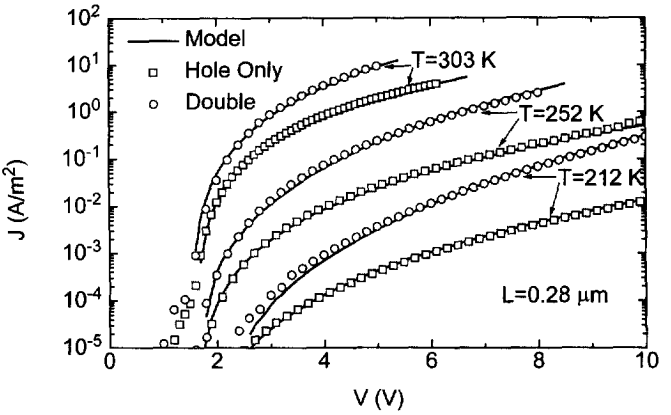

Fig. 6. Experimental and calculated (solid lines) $J-V$ characteristics for an ITO/PPV/Au hole-only device (squares) and an ITO/PPV/Ca double-carrier device (circles) with a thickness of $L = 0.28\,\mu$m at $T = 303$ K, $T = 252$ K and $T = 212$ K. The double-carrier $J-V$ characteristics are corrected for a built-in voltage V_{bi} of 1.5 eV which arises from the work function difference between the ITO and the Ca contact. The hole-only device is modelled using SCLC in combination with a field dependent mobility according to eqs. (2) and (3), the double injection current is numerically solved from eqs. (7) to (9).

and the particle-conservation equations

$$\frac{1}{e}\frac{dJ_n}{dx} = -\frac{1}{e}\frac{dJ_p}{dx} = Bp(x)n(x). \tag{9}$$

In the above equations, $p(x)$ and $n(x)$ represent the density of mobile holes and electrons, $n_t(x)$ the density of trapped electrons, and $E(x)$ the electric field as a function of position x. For the boundary conditions we assume that the injection is diffusion limited [8]. Furthermore, the electron trap distribution $N_t(\xi)$ as a function of energy ξ is assumed to be exponential with a characteristic energy kT_t, according to eq. (6). To determine $n_t(x)$ we assume quasi-equilibrium between the trapped and free electrons [9]. The set of eqs. (7) to (9) can be solved numerically.

As stated above the double-injection current now only depends on the bimolecular-recombination strength. The experimental results in Fig. 6 for the double-carrier device can be modelled from eqs. (7) to (9), with B as the only unknown parameter. These theoretical results are plotted as solid lines in Fig. 6. Clearly, our theory is in good agreement with experiment over a large voltage and temperature range. The obtained values for the bimolecular recombination constant B are shown in an Arrhenius plot in Fig. 7. For our present PPV device ($L = 0.28\,\mu$m) $B = 2 \times 10^{-12}$ cm^3/s has been obtained at

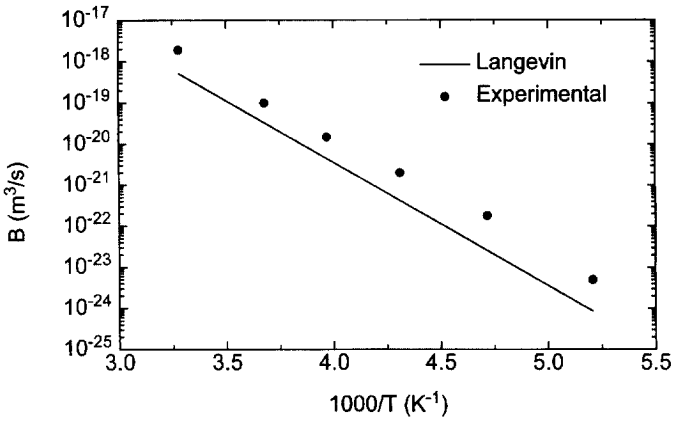

Fig. 7. Temperature-dependence of the bimolecular recombination constant (circles) as directly obtained from the $J-V$ characteristics as shown in Fig. 6 using the device model defined by eqs. (7) to (9). Also shown is the temperature-dependence of the Langevin bimolecular-recombination constant (solid line) as predicted by eq. (10) with $\mu_n = \mu_p$.

room temperature. We observe that B is thermally activated with an activation energy equal to that of the charge carrier mobility [18]. This result strongly indicates that the recombination strength in a PLED is of the Langevin type [19], i.e. diffusion controlled. Such a behaviour is characteristic for materials in which the mean free path of the charge carriers is smaller than a critical distance $r_c = e^2/4\pi\epsilon_0\epsilon_r kT$ at which the Coulomb binding energy between an electron and hole equals $-kT$. For an organic hopping system with a low carrier mobility the bimolecular recombination mechanism is expected [20] to be of the Langevin type and has recently been included in an analytical model for PLEDs [21]. In our PPV the mean free path is approximately equal to the distance between the conjugated sites which is of the order of 10 Å, whereas $r_c = 185$ Å at $T = 300$ K ($\epsilon_r = 3$). As a result the rate-limiting step in the bimolecular recombination process is the diffusion of electrons and holes towards each other in their mutual Coulomb field. This implies for the recombination [19]

$$B = \frac{e}{\epsilon_0\epsilon_r}(\mu_n + \mu_p), \tag{10}$$

which is also plotted in Fig. 7. The B as determined from our $J-V$ characteristics are slightly (factor 3 to 4) larger than the values predicted by eq. (10). A possible explanation for this small discrepancy might be the fact that recombination from trapped electrons may play a role as well [22].

It should be noted that by including Langevin recombination [eq. (10)] into eq. (6), the double-carrier current J becomes proportional to $(\mu_n\mu_p)^{1/2}$, which for $\mu_p = \mu_n$ implies that J is proportional to μ_p instead of $\mu_p^{3/2}$. An equal temperature dependence for the hole-only and the double-carrier device is the result, in agreement with the experimental results shown in Fig. 6. In fact, the temperature independence of the difference between the single- and double-carrier current is a direct demonstration that the recombination process is proportional to the charge-carrier mobility.

6. Device efficiency

Our model calculations reveal that the recombination efficiency in a PLED resulting from Langevin recombination approaches unity, making PLEDs efficient devices. The total number of recombination events inside the PLED as determined from the $J-V$ characteristics has been compared with the actual light-output. Only 5% of the total recombination contributes to the light output of the device. This is in agreement with the estimate that due to spin statistics the maximum electroluminescence (EL) yield cannot be more than 1/4 of the photoluminescence yield [3], which amounts to 15% for our PPV. The recombination processes in a PLED are thus mainly nonradiative. By taking into account out-coupling losses the internal efficiency of 5% is further reduced to an external quantum efficiency of 2 to 2.5%. In Fig. 8 the measured external conversion efficiency CE, defined as photon/charge carrier, is shown for a ITO/PPV/Ca PLED with $L = 0.11\,\mu$m at various temperatures. It appears that the CE of a PLED is independent of the temperature, in contrast to conventional semiconductor LEDs. This typical behaviour of a PLED is a direct consequence of the occurrence of Langevin recombination. In a space-charge limited device the number of charge carriers is mainly determined by the applied voltage and not by the temperature. As a result the device current is only dependent on temperature by means of the charge-carrier mobility. Since the recombination mechanism is of the Langevin type, both the recombination strength and the device current are thermally activated by means of the charge carrier mobility. If one adds to this the fact that in PPV the photoluminescence efficiency is independent [23] of temperature in the range 200 to 300 K, it is clear that the resulting CE of a PLED must be temperature-independent.

Furthermore, from Fig. 8 it appears that the CE of a PLED is dependent on the applied voltage. This bias dependence can be explained by the presence of electron traps [23]. At low bias the electrons are trapped close to the electron injecting contact and the light emission results mainly from

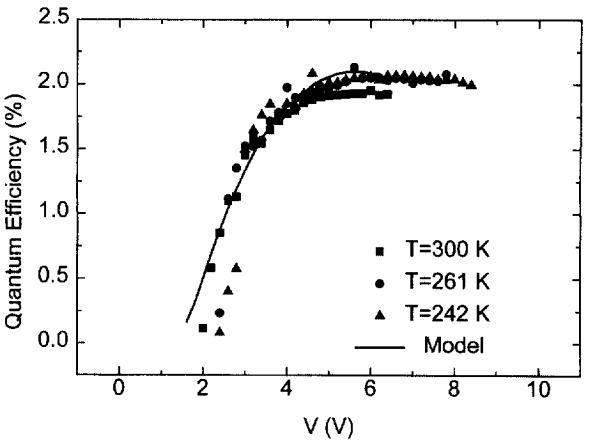

Fig. 8. External quantum efficiency (photons/carrier) vs. voltage measured from an ITO/PPV/Ca double-carrier device with a thickness of $L = 0.11\ \mu m$ at 300 K, 261 K and 242 K. The maximum quantum efficiency amounts to 2% and is independent of temperature. The calculated solid line includes interface losses.

the region directly adjacent to the metallic cathode. We suggest that the reduced efficiency at low voltage is a result of non-radiative recombination losses at the interface. With increasing voltage the electric traps are filled and the injected electrons penetrate further into the PLED, so that the device efficiency increases. This can be modelled by taking into account a 10 nm loss region at the cathode, which leads to agreement with experiment, see Fig. 8.

7. Enhancement of device performance

Our study has revealed several ways to improve the device performance of a PLED. Firstly, by decreasing the large amount of non-radiative recombinations the maximum conversion efficiency can be enhanced. Secondly, the use of an electron transport layer will shift the recombination zone away from the metallic cathode, resulting in an efficiency increase at low voltages. Due to the occurrence of Langevin recombination the device efficiency (light output/current) of a PLED is not dependent on the temperature. However, with decreasing temperature the voltage required to maintain a certain amount of light-output (or current) increases due to the decreasing charge carrier mobility, as shown in Fig. 9. As a result a PLED fabricated from a polymer with a low carrier mobility will only provide sufficient light-output at high

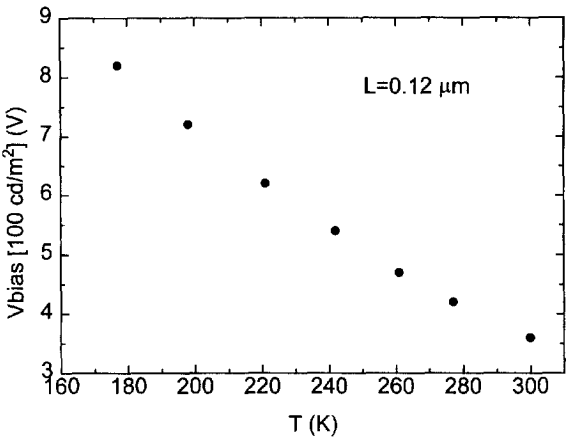

Fig. 9. Applied voltage at which the light outputs amounts to 100 cd/m^2 as a function of temperature. The observed voltage increase with decreasing temperature originates from the decreasing carrier mobility.

voltages, giving rise to a poor power efficiency. Thus for an optimum device performance both the photoluminescence efficiency and the carrier mobility of the polymer should be increased.

8. Conclusions

In general, we have demonstrated that the electron and hole currents in PPV devices with low contact barriers are determined by the bulk conduction properties of the polymer, and not by the injection properties of the contacts. The conduction of holes in a film of the conjugated polymer PPV is governed by a combination of a field-dependent mobility and space charge effects. The electron transport is limited by traps which are exponentially distributed in energy. A device model for PLEDs is proposed which demonstrates that the recombination in a PLED is mainly non-radiative, so that only 5% of the total number of recombinations contributes to the light output of the device. From the temperature dependence of the $J-V$ characteristics we have demonstrated that the recombination mechanism in a PLED is of the Langevin type. Due to this diffusion-controlled recombination PLEDs exhibit, in contrast to conventional inorganic LEDs, a temperature-independent recombination efficiency.

Acknowledgements

We are grateful to S. Breedijk, C.T.H.F. Liedenbaum, M.G. van Munster, and J.J.M. Vleggaar for their contributions to the work in this paper. We thank the European Commission (BRITE-EURAM contract "POLYLED" BRE2-CT93-0592 and ESPRIT contract "LEDFOS" 8013) for financial support.

REFERENCES

[1] J.H. Burroughes, D.D.C. Bradley, A.R. Brown, R.N. Marks, K. Mackay, R.H. Friend, P.L. Burn and A.B. Holmes, Nature **347**, 539 (1990).
[2] D. Braun and A.J. Heeger, Appl. Phys. Lett. **58**, 1982 (1991).
[3] D.D.C. Bradley, A.R. Brown, P.L. Burn, R.H. Friend, A.B. Holmes and A. Kraft, Electronic Properties of Polymers, Springer: Solid State Sciences 107, Heidelberg, 304 (1992).
[4] R.N. Marks and D.D.C. Bradley, Synth. Met. **55–57**, 4128 (1993).
[5] I.D. Parker, J. Appl. Phys. **75**, 1657 (1994).
[6] H. Antoniades, M.A. Abkowitz and B.R. Hsieh, Appl. Phys. Lett. **65**, 2030 (1994).
[7] D. Braun, E.G.J. Staring, R.C.J.E. Demandt, G.J.L. Rikken, Y.A.R.R. Kessener and A.H.J. Venhuizen, Synth. Met. **66**, 75 (1994).
[8] P.W.M. Blom, M.J.M. de Jong and J.J.M. Vleggaar, Appl. Phys. Lett. **68**, 3308 (1996).
[9] M.A. Lampert and P. Mark, Current injection in solids, Academic Press, New York, 1970.
[10] P.W.M. Blom, M.J.M. de Jong and M.G. Van Munster, Phys. Rev. B **55**, R656 (1997).
[11] D.M. Pai, J. Chem Phys. **52**, 2285 (1970).
[12] J. Frenkel, Phys. Rev. **54**, 647 (1938).
[13] H. Bässler, Phys. Status Solidi B **175**, 15 (1993) and references therein.
[14] H. Meyer, D. Haarer, H. Naarmann and H.H. Hörhold, Phys. Rev. B **52**, 2587 (1995).
[15] W.D. Gill, J. Appl. Phys. **43**, 5033 (1972).
[16] Yu.N. Gartstein and E.M. Conwell, Chem. Phys. Lett. **245**, 351 (1995); D.H. Dunlap, P.E. Parris and V.M. Kenkre, Phys. Rev. Lett. **77**, 542 (1996).
[17] P. Gomes da Costa and E.M. Conwell, Phys. Rev. B **48**, 1993 (1993).
[18] P.W.M. Blom, M.J.M. De Jong and S. Breedijk, Appl. Phys. Lett. **71**, 930 (1997).
[19] P. Langevin, Ann. Chem. Phys. **28**, 289 (1903).
[20] U. Albrecht and H. Bässler, Phys. Stat. Sol. (b) **191**, 455 (1995).
[21] J.C. Scott, S. Karg and S.A. Carter, J. Appl. Phys. **28**, 1454 (1997).
[22] P.E. Burrows, Z. Shen, V. Bulovic, D.M. McCarty, S.R. Forrest, J.A. Cronin and M.E. Thompson, J. Appl. Phys. **79**, 7991 (1996).
[23] M. Furukawa, K. Mizuno, A. Matsui, S.D.D.V. Rughooputh and W.C. Walker, J. Phys. Soc. Japan **58**, 2976 (1989).
[24] P.W.M. Blom, M.J.M. De Jong, C.T.H.F. Liedenbaum and J.J.M. Vleggaar, Synth. Met. **85**, 1287 (1997).

Authors Biographies

Paul W.M. Blom; Ir. Degree (Physics), Technical University Eindfoven, 1988; Ph.D., Technical University Eindhoven 1992; Philips Research Laboratories, Eindhoven, 1992–. His thesis work was on picosecond charge carrier dynamics in GaAs quantum wells. At Philips Research Laboratories he was engaged in the electrical characterization of various oxidic thin-film devices. From 1995 he is investigating the electro-optical properties of polymer light-emitting diodes.

Marc J.M. de Jong; Ir. Degree (Physics), Delft University of Technology, The Netherlands, 1992; Ph.D., Leiden University, The Netherlands, 1995; Philips Research Laboratories, Eindhoven, 1991–. He has worked on shot noise and electrical conduction in mesoscopic systems, on opto-electronic properties of polymer light-emitting diodes, and on sensors for automotive applications. His current activities are in the dield of broad-band communication and access networks.